UCRL-PROC-206061

LAWRENCE
LIVERMORE
NATIONAL
LABORATORY

Report on the Instrument Development Workshop for Biological Imaging Experiments at LCLS

Henry Chapman, Janos Hajdu, Keith Hodgson

August 16, 2004

Instrument Development Workshop for Biological Imaging Experiments at LCLS
Menlo Park, CA, United States
March 15, 2004 through March 16, 2004

Disclaimer

This document was prepared as an account of work sponsored by an agency of the United States Government. Neither the United States Government nor the University of California nor any of their employees, makes any warranty, express or implied, or assumes any legal liability or responsibility for the accuracy, completeness, or usefulness of any information, apparatus, product, or process disclosed, or represents that its use would not infringe privately owned rights. Reference herein to any specific commercial product, process, or service by trade name, trademark, manufacturer, or otherwise, does not necessarily constitute or imply its endorsement, recommendation, or favoring by the United States Government or the University of California. The views and opinions of authors expressed herein do not necessarily state or reflect those of the United States Government or the University of California, and shall not be used for advertising or product endorsement purposes.

Report on the Instrument Development Workshop for Biological Imaging Experiments at LCLS

March 15-16, 2004 at SLAC

Organized by Henry Chapman (LLNL), Keith Hodgson (SSRL) and Janos Hajdu (U. Uppsala)

Abstract

The Linac Coherent Light Source (LCLS) will launch a new era in X-ray science by providing 200 fs pulses of X rays with a peak brightness up to 10 orders of magnitude greater than current sources. One of the most exciting and far-reaching experiments that this new source will enable is single-particle diffraction imaging, whereby atomic-resolution structure of biological macromolecules, complexes, or viruses could be obtained without the need for crystallization. Time-resolved structures and dynamic processes could be studied, with time steps as short as the LCLS pulse duration. Many of the components of a diffraction imaging experiment have been demonstrated individually, such as image reconstruction and electrospray mass-spectrometer particle selection. There are many issues that cannot be resolved until bright pulsed X-ray sources become available in 2005 to test theories. Bringing all the techniques together to field an experiment at LCLS in 2009 is a challenging, but quite feasible, undertaking that requires a coordinated and sustained effort of the community.

1. Introduction

The Instrument Development Workshop for Biological Imaging Experiments at LCLS* was held on March 15-16, 2004, at the Stanford Linear Accelerator Center, in Menlo Park, California (Appendix A). The meeting was held to bring together the community of researchers who plan imaging experiments at LCLS and to identify the research priorities that must be undertaken before LCLS experiments can be fielded. The workshop was co-organized by Lawrence Livermore National Laboratory, University of Uppsala, and the Stanford Synchrotron Radiation Laboratory. Major support came from the SSRL Structural Biology Program (NIH NCRR and DOE BER), and the NSF Center for Biophotonics Science and Technology. The workshop was attended by over 60 people from universities and DOE and NIH national laboratories (see Appendix B). Over 15% of participants were from outside the US.

The meeting consisted of presentations and discussion to determine the research needs for single particle imaging, and other atomic-resolution imaging methods, to be carried out on the LCLS. These included briefings on critical aspects of the source, detectors, X-ray optics, sample handling, effects of rapid photoionization on image degradation, and data processing (classification of diffraction patterns, registration, and image reconstruction), among many other issues. These discussions were followed up

* See the glossary for definitions of acronyms.

with breakout sessions in each of the technological subsystems of the experiment, focused on project risks, mitigation strategies as well as milestones and costs (the latter were refined in e-mail discussions following the meeting). The overwhelming consensus at the workshop was that while much challenging research needs to take place to develop the required techniques, the community will be able to field the initial stages of experiments in X-ray free-electron laser (XFEL) imaging at the LCLS by the 2009 operations date.

The organization of this report closely follows the agenda of the workshop. The requirements of the XFEL pulses and other experimental parameters are summarized in Sec. 2. These requirements are according to our present understanding of the experiment and the physics of the interaction of high-peak-power X-ray pulses with small particles. Much of the program of research in the years prior to LCLS operations and in the first years of LCLS operations will be devoted to quantifying those experimental requirements and relating them to a straw-man layout of the LCLS experiment. The research also has to develop some of the technologies for LCLS experiments. These needs are discussed in Sec. 3, where the findings of breakout groups in each of the experiments' subsystems are presented. The subsystems include front-end optics, particle delivery and orientation, photon-matter interactions, detectors and diagnostics, and image reconstruction. The risks and prioritization of efforts are summarized in Sec. 4. The workshop agenda and list of participants are given in the appendices.

2. Goals and Requirements of the Experiment

The ultimate goal of the experiment is to obtain atomic-resolution 3D electron-density maps of reproducible biological materials that cannot be crystallized. This is done using a supply of identical particles, with a strategy much like single-particle cryo-electron microscopy. In the simplest, but most challenging, experiment, each particle is injected into the path of an XFEL pulse and the coherent X-ray diffraction pattern from that pulse is recorded. The particle will have been at a random and unknown orientation. Many single-pulse diffraction patterns are classified into groups of like-orientations and averaged to achieve the required signal to noise ratio (SNR). Then the orientations of the classes are found with respect to each other by computations. By taking advantage of the oversampling of the diffraction intensities (and any other available information about the object), the phases of the diffraction amplitudes are found by computations, enabling the determination of a 3D image. Since the diffraction data is recorded with such a brief pulse of X-rays, time-resolved structural information can be readily achieved—for example initiating a photoreaction with a visible laser pulse synchronized to the XFEL. Earlier considerations of the experiment were developed as part of the scientific case for the LCLS and the Tesla FEL and can be found at http://www-ssrl.slac.stanford.edu/lcls/papers/ lcls_experiments_2.pdf and http://xfel.desy.de/content/e169/index_eng.html, respectively.

2.1 Requirements for the experiment

The requirements for the single-particle experiment to be carried out in all generality are based on current models. We assume a resolution of 4 Å for a ~50 to 300 Å-radius molecule:

Pulse fluence: This is determined by the signal to noise ratio required to classify a diffraction pattern to a given resolution. Typical numbers are 10^{11} to 10^{13} photons per 100 nm spot, for 5 fs duration. Fluence could be reduced for highly symmetric particles, pre-oriented particles, or 2D arrangement of particles. The required fluence is proportional to photon energy.

Pulse duration: This is determined by the degradation of resolution due to sample damage. Current estimates are 5-10 fs at 8 keV for 5Å resolution and a fluence of ~10^{11} photons/(0.1 micron)^2. The duration can be increased if the experiment allows reduced fluence, e.g. for symmetric particles and the other cases mentioned above.

Pulse jitter: This is determined by the requirements of the particle injection system. For example, if the sample moves at 10 m/s, it will remain in the 0.1 micron interaction volume for 10 ns. The pulse jitter, and the jitter of the injection system must be considerably less than this, or about 1 ns.

Number of diffraction patterns: This is dependent on orientation of particle (whether it can be influenced), symmetry, and prior knowledge about the object. Typically 10^3-10^4 patterns per view are required, with 100 to 1000 views (ie 10^5-10^7 patterns total), in the case when there is no prior knowledge.

Bandwith of pulse: The inverse bandwidth, $\lambda/\Delta\lambda$, must be greater than or equal to the number of independent pixels in one dimension, or (2 * diameter of object)/(resolution). For example, for 0.4 nm resolution of a 30 nm object a bandwidth of 150 (0.7%) is required. A shot-to-shot variation in wavelength greater than this is tolerable, as long as it is measured on each pulse so the diffraction data can be appropriately scaled. High-harmonic contamination is acceptable at less than the 5% level.

Photon energy: The optimum photon energy to achieve maximum signal for minimum dose is between 6 and 14 keV. Initial low-resolution experiments may be at 4 or 2 keV where higher scattering cross-sections will lead to more sensitive measurements of damage. Note that LCLS provides a greater number of photons/pulse at lower energy (2×10^{13} at 0.8 keV, compared with 2×10^{12} at 8 keV). The number of scattered photons per independent pixel in the diffraction pattern increases proportionally with wavelength, λ, but for the same pulse energy the damage increases faster than λ since less electrons escape the particle. Initial calculations show that for the same number of photons per pixel the damage is fairly insensitive to photon energy below 8 keV.

Transverse coherence: This is required to be able to use entire beam (focused to a spot size comparable to the sample size) for recording the coherent diffraction pattern without needing to lose photons by spatially filtering the beam. Upstream optics should not distort the phase of the beam too much otherwise phase variations across the beam incident on the sample, may prevent a stable image reconstruction.

Vacuum: The background pressure must be $<10^{-9}$ mbar, for a tolerable amount of non-sample scatter adding noise to the diffraction pattern.

2.2 Reduced requirements experiments (for initial LCLS parameters)

The requirements of pulse duration and fluence will not be satisfied by the LCLS nominal parameters at initial operations (see Sec. 3.1). The ~5 fs required pulse duration will be most challenging to meet. X-ray optical pulse compression schemes (see Sec. 3.1.2) will be put in place within the first two years of operation of LCLS, but even before these become available many experiments will be needed to be carried out as part of the R&D and commissioning of the final experiment. Foremost are measurements of the rates of damage of particles to provide the first direct tests of current models, and to better determine the pulse requirements for imaging single molecules. Imaging experiments will also be carried out in the early stages, in order to develop the techniques required for such extreme X-ray pulses and to provide scientific results. Biological imaging will be achieved by various strategies, including the use of 2D microcrystals, arrays of particles and nanocrystals. Besides the relaxed pulse duration, initial experiments will require 10 μm spot instead of 0.1 μm (i.e. 10^{-4} of the fluence). This also relaxes the requirements of the optics and the particle delivery system.

3. Instrumentation

The layout of the experiment will be of the same general form for initial tests and measurements as for the ultimate single-molecule experiments. A schematic of the instrument is given in Fig. 1. The instrument consists of a chamber into which particles may be introduced one by one or as a cloud or spray, such that one or many particles will interact with the incoming LCLS pulse. The focused LCLS beam diffracts from the sample, and the continuous diffraction pattern is sampled on a pixellated detector (shown in Fig. 1 as two detectors—high-angle and low-angle—that will be able to encompass the entire dynamic range of the diffraction pattern). The recorded intensity pattern must be read out after every pulse and stored. The strong direct beam passes through a hole in both detectors and an "intelligent beam stop" measures parameters of the energy and timing of the pulse. Information about how well the particle interacted with the beam (e.g. whether it was centered in the beam) could be determined from the diffraction data itself, various optical or electron/ion detectors, or a mass spectrometer that measures the degree of fragmentation of the particle. Integral to the instrument is the image reconstruction algorithms and computer hardware to carry this out. Diffraction data must be classified, averaged, and combined into a 3D dataset to be reconstructed by phase retrieval. Other subsystems could include a laser-based or electrostatic trap to briefly hold the particle in the interaction region, and a high-field elliptically polarized laser to orient the particles.

A recommendation of the workshop is to develop and publish a straw-man design of the single-particle diffraction imaging experiment. This will enable the teams working on the various subsystems or on developing methods to work towards common goals and to remove uncertainties on how design decisions on one subsystem will impact other systems. The straw-man layout would include realistic beam parameters, all necessary optical elements (including beam diagnostics), the sample, and detectors for measuring the diffraction pattern itself. Given the straw-man layout a full experiment could then be

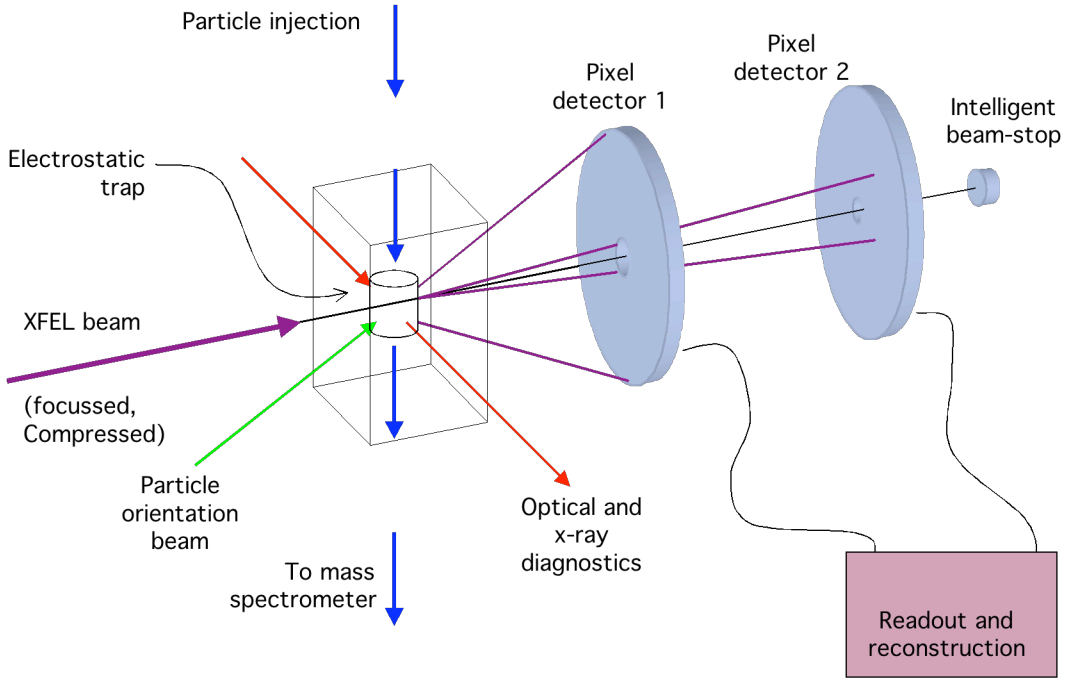

Fig. 1: A schematic of the single-particle diffraction imaging experiment.

realistically simulated, including reconstruction, so that the allowable signal to noise ratio (SNR) could be evaluated. The straw-man evaluation is important for helping design each component of the experiment. Even beam diagnostics potentially may add noise to the experiment so they must be designed within the scope of the entire experiment. The straw-man evaluation would be an ongoing process that would be updated and validated where possible with experiments performed on interim sources such as the SPPS and the Hamburg VUV-FEL.

In the subsections that follow each one of the instrument subsystems is outlined and the current understanding of the research requirements, project risks, mitigation strategies, and costs are given as determined during the workshop discussion and breakout sessions. The physics of the interaction of XFEL pulses with single particles is considered a subsystem in this context, since this drives the requirements of the other subsystems and determines the bulk of the R&D leading up to LCLS operations.

3.1 Front-End Optics and Diagnostics

The front-end optics are those required and provided for by the experiment and do not include the beam delivery system of the LCLS. For reference, details of the LCLS source parameters can be found at the LCLS home page [1], and details of possible source upgrades are given in [2]. The nominal pulse parameters of LCLS are 120 Hz repetition rate; 230 fs FWHM duration (67 fs RMS variation); 2×10^{12} photons at 8 keV photon energy; 0.05% single-shot bandwidth; 0.21% shot-to-shot wavelength variation. The X-ray pulses can be provided with a wavelength chirp, which would allow pulse

compression with X-ray optical elements, but only if the diffraction imaging can tolerate the bandwidth that results. Options for chirping include a linear wavelength variation of: 0.5%, 1%, 2% (ie. 10, 20, 40 times homogeneous bandwidth). The front-end optics must provide a focused beam, at the sample, that satisfies the requirements of pulse fluence, duration, bandwidth, photon energy, and coherence as listed in Sec. 2.1. The optical elements must function reliably for at least as many as the 10^5 to 10^7 pulses required for a single experiment, and possibly orders of magnitude more than this, depending on the efficiency of the sample delivery system.

We address the questions and risks associated with the quality of the FEL photon bunch at the sample that is necessary to achieve single molecule imaging. Assessing the risks, and setting in place mitigation strategies, defines the elements of a front-end optics R&D plan.

3.1.1 Beam focus (spatial compression)

Sub-micron focusing of 8 keV X-rays is routinely achieved at synchrotron facilities. Several groups have demonstrated focusing of X-rays at better than the required 100 nm focal spot, using Kirkpatrick-Baez (K-B) mirror pairs. These include the ESRF group [3] (< 90 nm focus) and the Japanese group [4] (< 40 nm focus). Such high performance has been enabled by meeting the surface finish requirements over spatial scales from the size of the optical element down to submicron periods, and with active alignment based on X-ray wavefront sensing (such as the Hartman sensors developed by ESRF). The K-B mirror technology appears to be directly transferable to the LCLS, although there may be some risk of damage at the high peak power density of LCLS pulses (see also Sec. 3.1.5). Results from the Japanese technology, reported after this workshop, are very encouraging. Measurements of the beam intensity after propagation of 1 m showed ~10 % variation in intensity, which is close to that predicted. This was achieved with a RMS mirror surface error of 0.2 nm [5].

In general the K-B optics working distance should be as long as possible, to reduce scatter from contaminating the diffraction data. Note that since the source size in the undulator is <100 μm, the optical train needs to deliver a demagnification of 1/1000 for a 0.1-μm diameter spot. Without any relay optics, and a source to optics distance of 400 m, this places the focus 40 cm from the optics. A 1-μm spot requires a K-B working distance of ~4 m.

It is not yet known whether the current K-B mirror and sensor technologies meet the wavefront requirements of the single-particle diffraction imaging experiment. The uniformity of the wavefront is important in diffraction imaging: the 2D image reconstructed from a single diffraction pattern will represent the exit wave from the specimen, which is the product of the complex transmission of the sample with the incident wave. There would be no easy way to distinguish a phase variation in the image due to the beam or sample, and a phase variation in the beam may prevent reconstruction from converging. In 3D imaging, each diffraction pattern would need to be corrected for the imperfection of the incident beam before a full reconstruction; that would be difficult and time consuming. Current synchrotron-based diffraction imaging experiments overcome this problem by the use of a pinhole spatial filter placed between optics and the sample. We would want to avoid this in LCLS experiments due to problems with damage and scattering and since it removes a large fraction of the photons. A variation

of the wavefront from shot to shot may occur due to jitter in the source position in the undulator causing a change in illumination on the focusing optics, for example. The effect of such a variation on the SNR of reconstructed images, and the effect of a static wavefront variation across the sample, must be assessed using the straw-man geometry of the experiment.

Experimentally, the problem of shot-to-shot reproducible production of the same coherent wavefield at the submicron focused "probe" requires accurate characterization of the aberration function (or pupil function) of the probe-forming optics. Such methods are beginning to be employed in the characterization of K-B optics, such as the Hartmann sensor developed by ESRF. This problem has been confronted in the scanning transmission electron microscope (STEM) community, where fully coherent sub-nanometer probes are formed—which is carried out by a form of shearing interferometry. Details are given in [6]. The arrangement has been emulated in the scanning transmission X-ray microscope (STXM) [7]. A suitable large-period transmission grating to form the shearing interferometer might be formed from a multilayer cut normal to the layers (Laue geometry), and it may be possible to place this downstream of the sample and detectors, in the direct beam that passes through the hole in the CCD detectors. This process of wavefront optimization can be automated to generate signals which are fed back to the probe-forming optical elements. More details can also be found in a patent held by the Nikon Company and Spence and Zuo, Microdiffraction, Plenum, 1992.

3.1.2 Temporal compression and slicing of the beam

Temporal compression of the pulse from the nominal 230 fs to the required 10 fs or less is required. One method for reducing the pulse duration is known as time slicing [8,9], in which the total number of photons in the pulse is also reduced proportionally. An example of time slicing is to chirp the X-ray pulse (by chirping the energy of the electron pulse feeding the undulator) to give a correlation between photon energy and time along the pulse. Selecting an energy “slice” with a monochromator (such as a short-period multilayer) selects the corresponding time slice. This method is fairly straightforward and will be useful for intermediate imaging experiments (e.g. reduced spatial resolution). To use this method to provide short pulses with the as-required fluence would need the K-B mirror pair to compensate for the decrease in fluence by decreasing the focus area by a factor 20 or more (and also to improve the particle delivery accuracy by the same factor). Pulse compression with a conservation of a much larger fraction of the photon count could be achieved using an optical setup that delays the various photon energies of the chirped pulse. Examples include a grating pair, or a strained crystal, both of which are more complicated systems than slicing.

Care must be taken to minimize (preclude) energy outside of the 10 fs window; pre- or after-pulse effects can both affect target integrity and add noise to the diffraction pattern. Modeling can provide estimates of tolerable pre-pulse or after-pulse fluence. The compressor must be included in the SNR calculations using the straw-man geometry.

The required pulse duration might be alleviated by the implementation of various mitigation techniques including: tamping (providing a sacrificial low-Z material around the molecule such as encasing it in a helium drop); imaging samples with high symmetry; or orientational alignment of the sample.

3.1.3 Beam bandwidth

The system SNR calculations using the straw-man geometry should include possible harmonic and spontaneous irradiation profiles. If necessary, multilayer coatings may be used to remove or reduce these components.

3.1.4 Wavefield coherence

Diffraction imaging requires that the wavefield be coherent across the extent of the sample. Since the LCLS beam is fully transversely coherent, this will be the case. Note that optics, even those with rough surfaces, do not reduce beam coherence but can cause variations of the phase (or curvature of the wavefront) that will have the effect of reducing the contrast of diffraction patterns. Thus a thorough understanding of these effects must be developed (see also 3.1.1). The capability of measuring the contrast of diffraction patterns from test objects should be provided in the experiment, to diagnose the effective degree of coherence at the sample. Ideally, the mutual coherence function of a single pulse would be measured, using Young double slit interferometer [10], diffraction from uniformly-redundant arrays [11], or other interferometric techniques [12, 13, 14].

3.1.5 Optics Reliability

The diffraction imaging experiment will be conducted in the far experimental hall, about 400 m from the source. Where the experiment and optics will be located the average intensity is 0.6 J cm^{-2} which is comparable to today's undulator sources. Cooling will be required, using methods currently employed at third-generation sources. The peak fluence is of more concern. Even though calculations show that standard optical elements with standard materials are permissible, the sub-ps regime is new, and experiments are warranted. It is important to perform these at the relevant photon energies. A laser-driven $K\alpha$ source and the focused SPPS beams are candidates.

3.1.6 Diagnostics

The photon bunch diagnostic measurements required are: photon energy, photon bunch duration (time), intensity spatial profile and pointing, bandwidth, wavefield coherence, and wavefront geometry (phase). The experimental requirements on accuracy, etc. remain to be specified. All except wavefront phase, and the pulse length at the required temporal resolution of sub 10 fs, are being made available by the facility, in principle on every shot. The wavefront phase can be reconstructed by multiple measurements of the intensity profile along the beam path; this capability will exist. Measuring the X-ray pulse duration to sub 10 fs resolution [15] is challenging and should be considered an FEL and X-ray community project. Note that some of these diagnostics should be positioned both upstream (a long way to reduce noise) and downstream of the experiment, and should be included in the straw-man design.

3.1.7 Plan for front-end optics and diagnostics

Task 1: Model the effect wavefront aberrations (over a length scales from the atomic scale to the size of the object) on imaging, using the straw-man experiment with inputs from detailed characterizations of current optical surfaces. Requires 1 FTE.

Task 2: Design and commission a K-B system for the LCLS experiment. Existing and future developments of K-B systems for LCLS should be fully characterized and compared with models. In addition, the requirements of wavefront characterization techniques must be specified (through the straw-man calculations) and these techniques must be further developed. Requires $1M and 5 FTEs.

Task 3: Temporal pulse compression is considered a high risk, and early assessment is very important. More than one route to temporal compression should be followed. An R&D effort should begin immediately, with the objective of building a temporal compressor, and testing it at SPPS. R&D aimed at alleviating the required pulse durations needs to be initiated as soon as possible. Requires $200K and 4 FTEs.

Task 4: Develop techniques to diagnose the effective degree of coherence at the sample. Requires 1 FTE and $50K.

Task 5: Initiate R&D to demonstrate the reliability of the optical elements in the high-fluence sub-ps regime. Requires $100K and 2 FTE

Task 6: Initiate R&D to develop diagnostics for pulse length at the required temporal resolution of sub 10 fs, and develop technique to measure wavefront phase. Requires 3 FTEs.

Task 7: Design and commission a zone-plate imaging system to provide low-resolution images concurrent with the diffraction data. Requires $200K and 1 FTEs.

Optics budget: 17 FTEs and $1,550K

3.2 Particle Delivery Systems and Orientation

One of the biggest experimental challenges in biological imaging with LCLS is the need for containerless samples. Since the quantities of material of the sample under study will be so minute, there should be no (or very little) other matter in the beam. When imaging single molecules, the sample cannot be held on a substrate, since scattering from the atoms of the substrate will overwhelm the signal of the molecule itself. In addition, the sample region must be at ultra-high vacuum of $\sim 10^{-7}$ mbar or better (note that a pressure of 10^{-7} mbar corresponds to ~ 280 residual gas molecules in a path length of 100mm with diameter 1 mm). Therefore, particles such as macromolecules or virus particles must be injected from the outside into the x-ray beam in such a way that single particles intersect with the brief XFEL pulses. While it would be ideal to inject one fresh, single particle into every focused x-ray pulse at a 120 Hz rate in the LCLS this would require precise control of the particles' trajectories both in space (< 1 μm) and time (< 10 ns). Such a precision exceeds current sample injection and particle manipulation capabilities by several orders of magnitude and it is clear that present single particle manipulation techniques need to be improved significantly. One of the key efforts of this project will

be on improving single particle trajectory control capabilities in order to advance to precision single particle introduction schemes.

As the particle introduction and manipulation techniques mature further in the near future, we expect that it will become possible to inject few or even single particles into the beam at the proper times with well-controlled velocities or by trapping single particles at the XFEL beam focus using optical or electrostatic methods. A promising avenue of research is the development of water or liquid helium droplet sources, as being undertaken at Arizona State University. A solution of proteins is introduced into vacuum through a small orifice. The cylindrical stream energetically favors forming into drops of constant size and spacing (the Rayleigh instability). The fluid drops cool rapidly due to the decrease in pressure when introduced into vacuum (superfluid helium drops may be formed) and the drops sublime at a constant rate giving a way to control the drop size. If the drops can be controlled to the required precision this will be an attractive sample introduction method, since it also provides a sacrificial layer (or tamper) that may delay the rate of explosion of the molecule.

An alternative and possibly simpler approach that will be developed in parallel for the initial experiments at LCLS is the "shot-gun" introduction of bursts of particles. In addition to Rayleigh drops and the shot-gun approach we will also explore the introduction of regular arrays of aligned molecules attached to ultra-thin membranes or small, symmetric scaffolds. The shot-gun and array approaches are described in more detail in the following.

3.2.1 "Shot-gun" introduction of particles

For the initial experiments at LCLS, proper particle positioning could be achieved by injecting short, concentrated bursts of particles into the beam focus area and relying on statistical spatial and temporal alignment of individual particles. This "shot-gun" approach requires shot-to-shot diagnostics to determine whether a particle was properly aligned with respect to the x-ray beam. Such diagnostics could be provided, e.g., by a mass spectrometer that analyzes the fragments of the particle after the x-ray shot passes through. This shot-gun approach can use existing pulsed electrospray techniques to create busts or "puffs" of particles or molecules. However, the required particle densities are quite high and space charge effects need to be overcome in achieving sufficient local particle density near the x-ray focus.

Particle Creation by Electrospray Ionization:

Electrospray ionization (ESI) and related ink-jet spraying techniques are a convenient way to bring single, large molecules or small particles, such as viruses, from a storage solution into the gas phase [16] and we will explore the use of these techniques for our purpose. Those spraying techniques have been refined in recent years for their application in mass spectrometry of large proteins, supramolecular complexes, such as intact ribosomes [17], and even whole viruses [18]. Electrosprays produce monodisperse aerosols of particles that can range in size from 2 nm to 2 micron. Electrospraying large biomolecules typically creates a distribution of charge states (roughly 1 charge per 1000-2000 Da molecular weight). While charge on the molecules is convenient for manipulating their trajectory, too much charge may distort the molecular shape. If

desired, the charge on the molecules can be reduced to a few elementary charges using a (partial) neutralizer or by using charge reduction ESI [19].

Selection of charge state and molecular conformation by Ion Mobility Spectrometry:
Once a distribution of charge biomolecules in the gas phase has been produced by ESI it is desirable to select a specific charge state and a specific molecular conformation for the diffraction imaging. Ion Mobility Spectrometry (IMS) is a convenient and fast tool for this selection process. In IMS, a pulse of charged molecules is injected into a drift tube filled with low pressure (~few Torr) gas where water and loosely bound adducts are quickly shed by the molecules. The molecular ions diffuse through the drift tube pulled by an electrical field and the ions are separated by their cross sectional area and their M/z state. Typical drift times are of order milliseconds. Molecular ions of the same M/z state and the same conformation arrive at the far end of the drift tube at the same time and pulsed gate electrodes can be used to transport those ions further into the x-ray beam line and to block all other ions with other composition, conformations or charge states. The use of an IMS stage thus provides sample cleanup, adduct removal and precise conformational control of the molecular ions to be diffraction imaged.

Particle Introduction into Vacuum:
One of the challenges in introducing particles or molecules from a storage solution at atmosphere pressure to the x-ray beam focus is to pass the particles into the ultra-high vacuum of the beam without spoiling this vacuum with residual gas or water vapor. For the particle introduction into ultra-high vacuum, we will expand on the aerodynamic lens or nozzle techniques used for single-particle mass spectrometry [20,21] and bioaerosol mass spectrometry (BAMS) developed at LLNL by some of us and by other groups. In aerosol mass spectrometry, single aerosol particles are sampled directly from air at atmospheric pressure and introduced as a focused particle beam into the high vacuum of a time-of-flight mass spectrometer through a nozzle expansion or an aerodynamic lens. A series of skimmers below the nozzle and differential pumping help maintain the high vacuum inside the system required for the mass spectrometer operation. If a combination of ESI and IMS is used for ion generation and preselection, the interface between the end of the IMS stage and the ultra-high vacuum of the XFEL beam line is already at a reduced pressure and molecules will have shed most of the attached water, facilitating the transition into the UHV of the beam line. As recent work by the groups of David Clemmer and Martin Jarrold have shown, pulsed ESI-IMS can be interfaced with a time-of-flight mass spectrometer vacuum system. Similar concepts can be employed together with some of the techniques used for BAMS for coupling and ESI-IMS stage to the XFEL beam line.

Particle Manipulation
In the ESI process, the particles are imparted a charge that is convenient for manipulating the particles in the gas phase by electrostatic forces. Consequently, most of the recent wall-less sample preparation methods use charges and electrostatic forces to constrain particles [22] (Bogan and Agnes 2002 and 2004). For the initial shot-gun type approach, synchronizer electrodes can be used, e.g. at the interface between the IMS stage and the UHV beam line or inside the beam line vacuum, to accelerate or decelerate a packet of

molecular ions exiting the IMS stage in order to fine tune the synchronization of the packet with an x-ray pulse. Similarly, buncher electrodes can be employed to briefly compress the packet of molecular ions to the densities required for sufficient statistical alignment with the x-ray beam (~10^{10}-10^{12}/cm^3).

One technique that may be useful for the manipulation of single particles or bunches of particles is charge-detection mass spectrometry. In charge-detection mass spectrometry recently developed by W.H. Benner et al. it was demonstrated that the charge on a large molecule or s single viruses can be measured by the particle through a Faraday tube coupled to a sensitive charge amplifier [23]. Such a charge detector can also be coupled to an ion trap for improved charge measurement [24]. An ion trap will also provide a convenient way to store charged particles for some time and to inject particles with tuned velocities at controlled times into the XFEL beam. Future integrated precision delivery systems for single particles may employ a charge detector in combination with an ion trap to control and manipulate the particles to be imaged in the x-ray beam.

Finally, we will also explore optical methods for manipulating and molecules or particles, such as "optical tweezers", which could be used to hold and potentially orient biological samples for a short period of time [25](Grier, 2003). When used with ultra-fast pulse x-ray sources, the thermal damage due to the tweezers will take longer to manifest than the damage due to the pulse itself. However, one concern with such optical tweezers is the potential distortion of the molecular conformation by the strong electrical fields involved.

3.2.2 Regular, symmetric arrays of molecules or particles on an ultra-thin substrate or scaffold

In addition to the shot-gun introduction approach, we will explore arraying multiple copies of identical particles (that are constrained to the same orientation) into regular clusters. Such an array could be produced, for example, on an ultra-thin, low-Z material membrane or by using a highly-symmetric virus capsid as a template to which molecules are attached in a symmetric pattern, as described further below. While such a thin substrate or a virus template may contribute some scattered background x-rays, the diffraction signal from the array should be drastically enhanced compared to a single particle. This would potentially increase the achievable resolution. Larger arrays of such microarrays could be loaded periodically into the vacuum of the x-ray beam through a load lock system and "fresh spots" of the sample could be brought into the beam by means of stepping the array through the individual microarray positions.

One example of such an array could be similar to the sample holder used in cyro-electron microscopy, i.e., a ~500 Angstrom thick vitrious ice film with the sample proteins embedded. Proteins could be aligned during freezing e.g. by electrostatic forces or optical means and would remain aligned after freezing. A second example of this would be 2D regular arrangements of particles made by scanned probe nanolithography (SPN) methods. In SPN, an atomic-force microscope (AFM) is used to form a pattern of self-assembled monolayers (SAMs) that is commensurate with the size of macromolecular targets. The functionality of the SAM is designed to give site-selective binding to macromolecules. Deposition of the target macromolecules onto the pattern results in attachment into arrays with known positions and constrained orientations. As a third example, molecular arrays of known symmetry could also be built by attaching

proteins to virus capsids that have high symmetry (e.g. an MS-2 bacteriophage capsid with icosahedral symmetry). In general, orienting or symmetrizing the sample could well enable the imaging of smaller molecules.

Model calculations will be used to assess the expected background from x-rays scattered off the thin membrane or the scaffold that are used to hold arrays of biomolecules. Such model calculations will help to determine the optimal configuration of such arrays and the necessary precision for positioning and aligning biomolecules in these arrays.

3.2.3 Research Plan for Particle Introduction

Task 1: Build particle introduction test stages integrating a pulsed ESI source, an IMS stage or time-of-flight mass spectrometer (TOF-MS), and a pulsed laser (simulating the pulsed x-ray beam) into a UHV system. These test stages will be used to optimize the synchronization between particle bunches created by ESI and preselected by IMS with a pulsed beam. These will also be used to test the charged particle densities achievable with this concept, and can be used as a particle delivery system at X-ray sources for particle X-ray scattering experiments (e.g., for validation of damage models described in Task 4 of 3.3). Requires 10 FTEs and $850K.

Task 2: Develop and test a Rayleigh droplet source. Determine properties of the droplets, including particle concentration, steering accuracy and timing (by detecting scattering of a pulsed laser). Test tamper concepts for delaying the Coulomb explosion at the VUV-FEL or SPPS. Includes nozzle fabrication. Requires 6 FTEs and $650K.

Task 3: Develop and demonstrate laser alignment of particles. Test with X-ray diffraction at synchrotron sources, and at SPPS or the VUV-FEL (which may required beamline modifications). Determine laser power requirements for particle sizes and degree of misalignment. Develop diagnostics that could determine orientation of misaligned molecules. Requires 10 FTEs and $1,100K.

Task 4: Develop methods to produce 2D arrays of molecules (including AFM methods, membrane systems such as vitreous ice membranes, and nanofluidic delivery of particles) and 3D nanocrystals. Test with X-ray diffraction at synchrotron sources and at SPPS or the VUV-FEL. Requires $300K and 8 FTEs.

Task 5: Develop methods to trap particles, optically or electrostatically. Test and integrate into the test station. Requires $350K and 5 FTEs.

Task 6: Perform long-time-scale molecular dynamics computations on the reproducibility of particles. Validate with IMS or TOF-MS measurements. Requires 6 FTEs.

Task 7: Develop concepts for pump-probe time-resolved experiments at LCLS with a particle injection system. Requires 2 FTEs and $200K.

Task 8: Develop diagnostics that will determine the centering of the particle in the XFEL beam (used to veto diffraction pattern readout). Requires $150K and 3 FTEs.

Particle delivery budget: 49 FTEs and $3,600K.

3.3 Development of a Predictive High Energy Density Photon-Matter Interaction Capability

The need for a computational capability that will provide a predictive behavior of an ensemble of atoms on the scale of a biomolecular object is critical for several reasons. First, the capability provides a method of determining the detailed experimental parameters in a much more cost-effective manner than performing an empirical experimental search. When the capability exists it can provide guidance on existing experiments to help determine the best set of parameters taking into account the complex interplay of the many components. One can test novel hypotheses in a computer simulation more efficiently than one can develop a new experiment. Second, the computational capability will provide the experimentalists with a method to analyze the data obtained from observation. Here the computer model provides time dependent parameters to compare with the data and assist interpretation. Third, since the logic connections between the various components of such a model are threaded together by fundamental physical processes the capability will permit testing of various hypotheses relevant to the goal of X-ray imaging of bio-molecules prior to the existence of the LCLS. Indeed, the development of surrogate experiments to validate aspects of the model is one of the more difficult aspects of the development of a predictive capability. The need to develop a computer model and experiments to test the computer models relevance are central to the type of bootstrapping essential to creating a timely predictive model.

3.3.1 Definition of the experiment:

To define the requirement for the simulation capability we first outline the part of the experiment that has to be modeled.

1. An X-ray photon beam with pulse length of 250 fs or less, about 10^{13} photons, and peak brightness of ~ 10^{33} photons/s/mm^2/mrad^2/(0.1% BW) impinges on an ensemble of atoms
2. The ensemble of atoms is not periodic, has density near solid and is composed of lower atomic number elements. The size of the ensemble is in the range of bio-molecules.
3. The beam interacts with the ensemble causing photo-ionization of the inner and valence shells.
4. The atoms undergo Auger decay, and are subject to collisions by the free electrons.
5. The electrons can escape the ensemble as their energy can exceed the Coulomb force slowing them.
6. The resultant loss of electrons creates a non-neutral positively charged ensemble that becomes subject to disassembly due to repulsive forces. Thus, the atoms and ion move.

3.3.2 Simulation Code Requirements

To obtain a predictive capability of the experiment briefly defined above, a computational model must include at a minimum the following aspects:

1. X-ray absorption processes: both inner- and valence-shell
2. Atomic/ionic rate processes in a population kinetics description (Auger decay, elastic electron collisions, excitation and de-excitation by electrons, electron collision ionization / recombination, radiative recombination, radiative decay)
3. Time-dependent hydrodynamic expansion
4. Self-consistent electric field generation (electron trapping and Coulomb explosion)
5. Environment effects (chemical bond energies, effects of chemical bonds on rate coefficients, plasma screening effects)
6. Output of variables necessary for post-processing by reconstruction algorithms and for fundamental model comparisons.

3.3.3 Requirement for Consistency and Validation

The need to provide a predictive capability goes beyond the inputs, physical processes, and outputs. Consistency of the various approaches and eventual experimental validation is essential. In the ideal situation we would have a surrogate set of experiments that tested various aspects of the predictions by providing highly reliable, reproducible observations that could be directly compared to the simulations. However, this is not possible in the foreseeable future for several reasons. First, these simulations are required for experiments that have no analogs - it is in fact the novelty of the next generation light sources that makes this effort so important. Second, development of the simulation capability is only three years old [26,27,28] and the complexities of the physical processes require much further effort. Third, the number of approaches to the problem is currently limited to two - 1) Molecular Dynamics (MD) and 2) Hydrodynamics (Hydro). This is, in large part, due to the relatively short period of time since the inception of the concept of single particle continuous diffraction imaging on 4th generation light sources.

Without the possibility of more ideal experimental data from these experiments and without a full code development activity we must rely on two paths to provide predictive capability:

First, we must institute an effort in the area of code development and cross-validation. As there are currently no complete models we need to further develop the current approaches to bring them to a state where comparisons are meaningful. The use of inter-code comparisons is essential to provide guidance on the performance of existing capability, to illuminate deficiencies and motivate a focused development effort.

Second, barring the full LCLS experiment we must design and develop experiments that provide tests of the underlying physical models and experiments that exercise the predictive, or integrated aspects of the simulations.

3.3.4 Plan

Given the above brief discussion a plan of action has been developed.

Task 1. Improve Current Codes:
Over a period of two years we must bring the simulation capability to a state where comparisons can be made and preliminary experimental designs and data analysis can be performed. See Appendices A and B to this section. Requires 8 FTEs.

Task 2. Code Development:
Initially we will look at some alternative approaches to attacking the problem. Identified for this is the Particle in Cell type (PIC) approach and the coupled kinetics / Boltzmann method (Kinetics). This effort would occur at the outset of the program of work to ensure that the results can be folded in to the final Design code. Additionally, an effort will be necessary after the preliminary studies to treat the non-symmetric nature of the molecules of interest. In the opinion of those involved, the MD approach alone can not treat the scale of the biomolecules that will form the first set of experiment in the foreseeable future and may always be restricted. Thus work on the multi-dimensional version of the code is essential. Finally, the work on the Design code will be finished in time for the initial operation of the LCLS. These developments will depend and drive the simulation cross validation, See section C below. Requires 16 FTEs.

Task 3. Simulation Cross-validation:
In lieu of high quality experimental benchmark data, which do not exist, we will initially depend on simulation code cross-validation. The process is straightforward, but it requires a three-phased approach. First, we need to define the important parameters for comparison amongst the various codes. Here the effort is to ensure that the comparison provides as clear an indication of the various aspects of the code operation as possible – see Appendix C to this section (Code comparison variables). Next, a definition of a series of test cases is needed that illuminate the underlying physical processes. Here the codes must be used initially to attempt to isolate those regimes where the, usually subtle, interplay of processes reaches thresholds that reveal the physical process of importance. Second, after defining the cases to be simulated, a workshop will be held to compare the codes. At this stage the workshop will be used to motivate code development and encourage participation from other groups around the world. The calculations should be uniform so that direct comparisons could be made. However, the amount of work involved should not be underestimated as the data reduction is voluminous and it must be performed in a manner that allows the participants, once assembled, to interact with the analyzed data and work in real time on the issue. Third, the workshop itself will be an interactive process where each of the problems is discussed, differences are highlighted, solutions offered, and outstanding issues categorized. The outcome of this process will be a plan for code improvement and code development. This process of cross-validation should happen twice before the opening of the LCLS. Requires 14 FTEs.

Task 4. Experimental Design and Analysis:
One of the major advantages of the simulation capability will be the design and analysis of experiments. From the point of view of building a predictive simulation capability

there are two purposes for these experiments: 1) to test various concepts and gain insight into our understanding of the physical processes of importance, and 2) in lieu of the LCLS, to develop a set of surrogate experiments that can stress our simulation capability. The role of experimental design and analysis are somewhat distinct in that in the former one uses the simulation to create an experimental configuration which behaves in a particular manner, while in the latter the experimental observables must be compared to the simulation by the application of post-processing. The nature of the post-processing of the data is such that much additional work is necessary that is not directly related to the simulation.

The set of potential experiments will potentially include those at:

1. SPPS: 80 fs X-ray source with 10^7 photons at 8 keV.
2. VUV-FEL: ~100 fs VUV source with 10^{12} photons at energies from 40 to 200 eV
3. Short Pulse Optical Lasers: to create X-rays for rapid photoionization
4. Short pulse Optical Lasers: to create Coulomb explosion of molecules/clusters
5. Short Pulse Optical Lasers: to create ~ 80 eV laser for other surrogate experiments.

These experiments require 15 FTEs and $500K. Some of the equipment from the particle delivery tasks will be used here too.

Photon-matter interaction budget: 43 FTEs and $500K.

3.3.5 Appendices

A. Current Code Status:

The two methods currently used, MD and Hydro, include several features necessary for the required simulation capability. Here we provide a list of what is included in these codes.

The Hydro model includes photo-ionization, Auger decay and collisional ionization by the free electrons. It assumes a spherically symmetric electron spatial distribution and a description of the electric fields generated by the ionized electrons, which provides the electron trapping mechanism. The ion motion is also spherically symmetric. Environmental effects of electron screening on the fields is included. Due to the symmetry this model can handle molecules of large and small sizes.

The MD models, which have at least two versions, include a description of photo-ionization, Auger decay and collisional ionization by the free electrons (called secondary cascades). It includes a description of the molecule in some individual detail. The free electrons and ion motion are tracked. A field is generated in the molecule. There are chemical effects included through the description of bonds by a Morse potential.

B. Known Improvements:

The list of process that needs to be implemented in the models is given here in a rough order of their importance:

1. Environmental effects; (chemical bonding, effects of electron screening and chemical bonds on the collisional cross-sections, effects on Auger decay rates.)
2. Compton scattering and heating
3. Effects of bremsstrahlung as it provides a signal, hence it is a potential noise

mechanism.
4. Ability to treat nanocrystals as well as non-periodic structures. This may be particularly important for experimental surrogates.
5. Quantum effects
6. Non-linear interaction due to intense fluctuations in the peak photon flux.

C. Code Comparison variables:
To compare the various code capabilities one requires a set of output variables that all the codes provide for comparison. An idea of such a set is given here for illustration:

1. Ionization state as a function of time and space
2. Internal energy level populations as a function of time and space
3. Electron distribution as a function of energy, time, and space
4. Ion positions as a function of time and space
5. Electric field as a function of time and space

3.4 Detectors and Diagnostics

3.4.1 Detector requirements and design issues

Single-particle diffraction imaging experiments at the LCLS will place unusual and unprecedented requirements on X-ray detectors and diagnostics. The detector has to be able to accept the signal from the pulsed X-ray source with a repetition rate of 120 Hz. Both exceptionally large global and local dynamic ranges are required to record the diffraction pattern: The local dynamic range is on the order of 10^3 over a few pixels, and the finite point-spread function (PSF) of the detector is a major concern. Possibly, the PSF-modified data will need to be deconvolved. The global dynamic range is greater than 10^6 for a diffraction pattern of a single molecule at 2A resolution. At these resolutions, single photon sensitivity is required, so that quantum detection efficiency (DQE) near unity is needed.

Depending on the sample size, degree of oversampling, and image resolution, we anticipate that the number of pixels on the two-dimensional detector has to be in the range of 500 to 2000 in each linear dimension (for single molecule diffraction a width of 500 pixels will be sufficient, but studies on arrays and nanocrystals will need the larger pixel numbers). At a rate of 120Hz, a very large amount of data is generated, and a compression of the diffraction patterns will be necessary. The data transfer rate, real-time compression, and storage are concerns.

The physical detector size will be limited by the environment of the experiment. The imaging resolution determines the required included angle of the detector from the sample (equivalent to the numerical aperture of the fictitious lens it replaces; resolution is given by the ratio of the wavelength to the sine of the detector half-angle). If a small-pixel detector is used, it will need to be very close to the sample to capture the high-resolution part of the diffraction pattern, which makes the experimental setup difficult. A large detector could be placed further back, but this would place greater demands on the vacuum requirements since the increased path length would lead to a greater background signal due to scattering from residual gas molecules in the beam path.

Diagnostics will be needed to help in the alignment of the experiment and to prevent the direct beam from impinging on the detector. This could be accomplished with a low-power continuous wave laser beam that is collinear with the X-ray beam, or by providing upstream attenuators. When measuring molecule diffraction a beamstop will be impractical since it will cause too much parasitic scattering. Instead, the direct beam should pass through a hole in the detector.

3.4.2 Existing detectors and a possible detector solution

The workshop participants found it useful to review novel detector designs to determine if detectors of similar characteristics are in the process of being developed in other areas, and if the development efforts could be coordinated. The over-riding issue is achieving very wide dynamic range with single photon sensitivity at the very high repetition rate of the LCLS. Phosphor-based fiber coupled charge-coupled detectors (CCDs) are the mainstay of almost all diffraction experiments and satisfy many of the requirements of the LCLS experiments, such as wide dynamic range and single photon sensitivity. However, they are slow, with typical frame – frame times of seconds. The solution that has been adopted by CCD manufacturers has been to simply add more readout ports; 4 is now quite typical, and even 32 port CCDs have been made. However, the limitation is really not the number of ports, but the readout electronics. In order to be able to manage a large number of readout ports, the electronics have to be miniaturized and placed close to the CCD. This has not been done commercially, but has been done for some specialized applications by national labs, such as for astrophysics satellite applications such as the Supernova/Acceleration Probe (SNAP) at Lawrence Berkeley National Laboratory (LBNL) [29] and for high-energy physics projects such as those at Max Planck Institute Munich [30]. A direct way of developing this existing technology to satisfy LCLS needs is to take the existing readout electronics used in CMOS detectors and make a column parallel readout, whereby a channel of readout electronics is associated with one or a few columns of a CCD. Such systems will be able to readout 1k x 1k CCDs in a few msec at full 16 bit resolution. It is also worth noting that other technologies could be developed to satisfy LCLS needs, but the timescale would be longer, the costs higher and the risk substantially higher. For example, the workshop identified active pixel sensors (APS) as a useful route, but not with out very substantial development. APS systems have transistors in each pixel which at the crudest level provide amplification and switching. This development is happening in the high-energy physics arena, but years of development will be required before the low noise necessary for single photon sensitivity can be achieved. It is also not clear at present from a theoretical perspective whether this can be done.

The participants discussed one specific embodiment of a detector that fulfills the requirements listed above. The research and development costs and timeline are discussed below in Section 3.4.5. This is only one of many possible solutions based on fiber-coupled CCDs that the participants could envision. In this specific scheme, two detectors are used in series to extend the dynamic range while maintaining a good DQE. A possible setup is shown in Figure 1. The front detector would consist of a phosphor screen fiber-coupled to the detector. In this scenario the fiber bundle of the first (wide-angle) detector should not occlude the second (small-angle) detector. The taper angle

would be close to zero, and the only reason for tapering is so that there is space for electronics and wiring connections at the CCD plane.

The wide-angle detector could consist of a two by two matrix of CCDs, a total of 4 CCDs per detector slice, and these CCDs should allow column parallel readout with a 120 Hz frame rate. The total number of pixels would be approximately 2000 by 2000 with a pixel size of 30 micrometer at the faceplate, giving a faceplate that is 60 mm along an edge. This would place the wide-angle detector at a distance of 75 mm from the sample for 4-Å resolution at 8 keV photon energy. The relatively large pixels of this geometry are used to effectively improve the PSF, which would be improved further if pixels were binned (as required for smaller diameter samples). The individual CCDs of the two modules will be slightly offset to produce a small hole in the center, allowing light to pass on to the second module or the beam monitor. The wide-angle detector would have a hole around 10 mm width, and the downstream small-angle detector would have a 0.5 mm wide hole, or smaller. The small-angle detector will receive the highest intensity of the pattern. This detector will be of reduced DQE, which could be achieved by placing an attenuator almost in contact with the phosphor screen, or by using a lower efficiency phosphor.

3.4.3 Challenges and research needs for detector development

There are several issues specific to our LCLS experiments that need to be addressed. For the conversion using phosphor films, phosphor damage and decay are both potentially problematic although evidence from detectors for X-ray lasers and from positron emission tomography (PET) scanners show that there are solutions available. Also, it will be challenging to achieve the required PSF although again, measured PSFs for 1:1 fiber coupled systems at LCLS energies look like they should satisfy the experimental requirements. Further, due to the low signals at the wide angles, the DQE will need to be close to one, which puts severe limits on fiber optics tapers and potentially limits the dynamic range. In addition, the detector environment and its impact need to be understood. Also, all LCLS specific geometry issues, such as tiling, pixel size, and placement of detectors need to be appreciated, which can be aided by the analysis of a straw-man design of the experiment. Finally, there is a need to design and simulate compression algorithms, hardwired in field-programmable gate arrays (FPGAs), for specific cases to determine if the data rate is sufficient. As opposed to crystallography, simple compression schemes cannot be used due to the non-crystalline nature of the samples. However, it may well be possible to fit the overall 2D scattering shape with a simply described polynomial for background, and then export only the small deviations from this value; this would result in significant compression.

Past experience has shown that there are two other issues with detector development in general. First, funding is not allocated at the appropriate rate because the detector is just assumed to be in place at the right time, and second scope creep. In this early phase of the experiment, the concrete experimental setup is not clear yet, and continuous learning refines our understanding of the detector requirements. However, modifications of the list of detector requirements could possibly have dramatic impact on the development of the detector technology and should be avoided if possible by any means.

3.4.4 Additional equipment

The discussions in the detector workgroup primarily focused on detector and readout issues. It was appreciated, however, that further diagnostics will be required, including a way to check the beam intensity, to detect if a molecule was hit, and means for low resolution imaging of the molecule. An "intelligent beam stop", consisting of a spectrometer or timing diagnostic would be of great benefit to the experiment.

3.4.5 Detector research plan: budget and timeline

In contrast to the historically rapid development of X-ray sources, the development of detectors for synchrotron radiation has been much more modest. Substantially detector technology development is necessary to meet the stringent requirements of our experiment. We anticipate that $2.5M over 18 months are necessary to develop a standard fast single-module CCD that meets the requirements. The majority of this money will go toward development work, and a replication of the CCD will cost $0.5M – $1M (two will be needed). Additionally, $2M over 18 months is necessary to develop a single four-quadrant detector and the hardware for the data compression (FPGA) and transmission.

Detector budget: 25 FTE and $6,500K.

3.5 Reconstruction Computations

Single-particle X-ray diffraction imaging will be performed by collecting a large number (10^5 to 10^7) of noisy coherent X-ray diffraction patterns, in series, from a supply of identical biological particles. One diffraction pattern is collected per particle and, in the most "basic" experiment, the particle will be at a random and unknown orientation. The reconstruction problem is that of deducing the real-space image that gives rise to this collection of (reciprocal-space) diffraction data. Since we are seeking to minimize the effects of radiation damage, by the method of flash imaging, we must develop methods that can use the lowest possible incident fluence per pattern. Due to the inherent power spectral density of spatial distributions of matter, the diffraction intensity decreases rapidly with increasing scattering angle, (corresponding to increasing resolution). That is, at the highest resolution of interest, the measured diffraction pattern is weakest and the number of counts per pixel in a measurement at this resolution will be less than one.

Image reconstruction will be accomplished through the general notions of (1) classification of the diffraction patterns into those where the particle had similar orientation, averaging within the classes to reduce the effects of photon shot noise (and any other experimental noise source), finding the relative orientation among the classes and (2) phase retrieval. While orientation classification and averaging of noisy diffraction patterns of unknown orientation has not yet been fully demonstrated, even on simulated data, the real-space version of this idea has been very successful in the field of cryo-electron microscopy. Once the averaged 3D diffraction dataset has been generated, the image can be obtained by phasing that diffraction data and Fourier inverting. For objects that have a finite size, or "support," the Fourier phases can be obtained by collecting data on a sufficiently fine grid—a concept referred to as oversampling—and processing that data with a phase retrieval algorithm. Although formally a unique

solution cannot be guaranteed, it can be shown, from the theory of factorability of polynomials of two and three complex variables, that ambiguities are highly unlikely with real objects. At least two classes of algorithms have been explored, and, in practice, they appear to be reasonably robust and tolerant to noise. Two- and three-dimensional reconstructions have been carried out on experimental X-ray diffraction data (Miao *et al*, others).

While the nominal fluence of the LCLS does appear to be adequate for the technique of single-particle diffraction, increased diffraction signals can be achieved by parallel imaging methods, such as the use of nanocrystals or 2D membrane crystals. These types of samples will be the focus of early discovery-class experiments at the LCLS while we learn how to deal experimentally with pulses of X-rays that are 10 orders of magnitude more intense than what we have experienced to date.

3.5.1 Requirements

As mentioned above, we can break the problem up into one of orientation classification and averaging diffraction data at random and unknown orientations into a 3D diffraction dataset, and one of reconstructing a 3D image. The averaging and reconstruction algorithms must be able to work with extremely noisy data and account for noise due to: photon quantization (including second-order correlations), inelastic scattering, scattering from optics and residual gas, pulse structure (bandwidth, temporal variation, and spatial variation), detector noise, and detector point spread function. The requirement on the signal to noise ratio (SNR) at the highest resolution is determined by the need to be able to determine whether a pair of diffraction patterns is of similar orientation, and possibly to determine if the patterns are from identical structures. The case of identical structures has been studied in the case of photon shot noise only (Huldt *et al* and Elser *et al*) and it is found that the number of detected photons per pixel can be much less than one. The incident fluence required depends on the object size and desired resolution, and ranges from 10^{11} to 10^{13} photons per 100-nm-diameter spot for large macromolecules. This compares with the expected 2×10^{12} photons per pulse expected from LCLS.

The number of diffraction patterns to be collected depends on the SNR required by the reconstruction algorithm, a requirement that has not yet been fully studied. To achieve a signal to noise ratio of five at the highest resolution will require 10^5 to 10^7 patterns in total. Reconstruction algorithms will be able to tolerate some missing data (e.g. diffraction blocked by the beamstop) when additional *a priori* information is supplied. The algorithms should make optimal use of the following information: object support, positivity, histogram of electron density (when available), atomicity (at the very finest resolutions), anomalous scattering, partial known structure, object symmetries, molecular dynamics refinements, and any other information that can be supplied by the experiment (e.g., a low-resolution image obtained by another means).

Algorithms must be parallelized and ported onto high performance computers. A single experiment of 10^7 patterns, each of 1024^2 pixels, corresponds to 40 Tb of data and could in principle be recorded in 24 hours of beamtime. The computing resources must be able to manage such a volume of data and to be able to process it at the rate of acquisition.

3.5.2 Possible reconstruction solutions

The orientation classification and averaging of a large number of noisy images of unknown random orientation has been successfully developed in the electron microscopy [31, 32, 33] community and software packages, e.g. SPIDER, exist. These could be adapted to reciprocal-space diffraction patterns (possibly an easier problem since the data do not have to be transversely aligned since the origin of the diffraction pattern is fixed). A new "merging" algorithm has been proposed by Elser that combines the classification and averaging into one step. This has many attractive features, such as providing a metric of progress and being easily parallelized.

The two types of image reconstruction algorithms are iterative transform algorithms and gradient search algorithms. The first category is represented by the widely used methods developed by Fienup [34], such as the Hybrid Input-Output algorithm. A solution is found by iteratively transforming between the feasibility sets of the measured diffraction magnitudes and a real-space support constraint, for example. The support constraint can be estimated from the measured data [35]. An example of the second category is the SPEDEN program [36] (Hau-Riege et al), which uses a constrained conjugate gradient solver to find an image whose Fourier magnitude is close to the measurement and imposed constraints. This program has the advantage that it only performs forward calculations and so can optimally deal with missing and irregularly gridded data. Also, built into the program is the use of object support, positivity, histogram of electron density (when available), atomicity (at the very finest resolutions), anomalous scattering, and use of any partial structure that is known. However, it is a local minimizer, so best results may be found with a global-searching iterative transform algorithm followed by refinement with SPEDEN.

3.5.3 Challenges and Research Needs

The biggest challenges are dealing with the huge volume of data that will be generated (processing it at the rate of acquisition) and in working with diffraction data with the minimum signal to noise. In addition, a challenge remains in demonstrating the technique of single-particle diffraction imaging including all the steps of orientation classification, averaging, and reconstruction. Robust algorithms must be developed and a large effort is required in producing software that can be easily and efficiently used for all aspects of data processing.

The former challenge should be addressed by developing parallel routines and testing on a smaller model object with available high-performance computers. Development must be done with the realization that this will be scaled to the full problem. The challenge of working with noisy data must be addressed both experimentally and theoretically. Here, experience must be gained with interim FEL sources, such at the Hamburg VUV-FEL, to determine and reduce or eliminate the sources of signal contamination that occur when working with a fully transversely coherent beam. Depending on the particle selection and delivery system there may be some variability of structure. For example, there may be several conformations of a molecule included in the dataset. While this variability must be quantified through molecular dynamics calculations and experiments, classification algorithms should be developed that can distinguish more than one particle variation as well as determining the orientations of each pattern for a given particle variation.

It might not be possible to resolve some issues until experiments are performed with pulses with all the parameters of the LCLS; proof-of-principle experiments must be carried out in the first operations of LCLS. The challenge of demonstrating the entire process of image reconstruction should be addressed with both simulated and experimental data. These tasks should be carried out by several research groups, in regular contact, in order to be able to come up with optimal strategies and algorithms. Experimental data takes a large effort to acquire and resources such as the VUV-FEL are extremely limited. Experimental data should be shared with all research groups to gain maximum benefit and the quickest progress.

Another research need is to determine how to make best use of data from additional diagnostics, such as an angularly resolved measurement of the charge of molecule fragments that are ejected by the Coulomb explosion, or a low-resolution (eg. 10 nm) image of the object formed by a zone plate lens.

There are a number of mitigation strategies that can be employed if the orientation classification method requires greater signal to noise on each measured pattern. The most promising are methods employing multiple particles in parallel, based on nanoclusters or nanocrystals, or 2D arrays of particles on a substrate. Even with less than 10 unit cells, the periodicity gives coherent addition at the Bragg positions. This strong signal can be used to more effectively classify patterns, which will be averaged, as above, to build up the non-Bragg signal. The ability to align particles that are injected into the beam will also affect the classification requirements.

3.5.4 Plan for imaging methods

The research plan necessarily follows the availability of source development. Beam time is allotted for biological imaging research at VUV-FEL in 2005 and following years. LCLS will be operational in early 2009. Experiments at synchrotrons have been ongoing, although more effort will be required to generate the datasets needed for algorithm and method development as well as to test equipment destined for VUV-FEL or LCLS.

Task 1: Develop full simulation of experiment, including noise sources. Determine experiment requirements, such as wavefront quality, detector PSF, pulse fluence. This is of low risk, but required for other tasks. We expect that it will take two persons for two years (4 FTEs). The completion of the task depends on X-ray interaction dynamics calculations (see section on X-ray matter interactions), as well as molecular dynamics calculations of reproducibility of samples.

Task 2: Develop and demonstrate efficient, robust classification and reconstruction methods. This task is of high priority, and low risk. It should be starting now (building on existing work, and use results of Task 1). It requires several groups, each possibly 3 persons/year (12 FTEs).

Task 3: Develop full software suite to handle and manage data volume, investigate and demonstrate deployment on high-performance computers (phased with available capabilities of computers). This is of low risk, the work should start FY05 with 3 persons/year. This task is dependent on Task 2. Requires $350K for a computer cluster and software, and 10 FTEs.

Task 4: Synchrotron-based experiments–2D and 3D, initially with radiation-resistant test objects. This is of low risk and is required for Task 2. It needs two or more groups of 4-5 persons/year for FY04-06 (total of 15 FTEs), transitioning to FEL experiments, and including testing of equipment to be fielded at FELs. It requires hardware and upgrades of $150K.

Task 5: VUV-FEL experiments: They are of high risk since there is a short deadline and there is no experience with such high brightness X-rays. It requires design, travel, hardware, and 6 persons/year for FY05-08 (18 FTEs). It includes 2D and 3D imaging experiments, and imaging of injected particles (e.g., simple clusters of colloidal gold particles).

Task 6: Design mitigation methods and try them out experimentally. It will occupy several groups, each of 1 or 2 people per year (12 FTEs).

Reconstruction budget: 71 FTEs and $350K

4. Alternative Methods

Several variations on the theme of diffraction imaging of single molecules were briefly discussed at the workshop. Two methods are described here:

4.1. Aligned molecules

Diffraction imaging of aligned molecules is easier than that of randomly oriented ones. On the simplest level, the number of possible orientations – for a given resolution - is diminished; therefore it is easier to determine the correct orientation of the particle than in a random ensemble. If the alignment is "perfect" the diffraction patterns can be always averaged correctly.

There are further possibilities to improve diffraction imaging of oriented molecules. The most general statement is that an array of well-oriented particles that are in random (disordered) positions is optimal for diffraction imaging. Its diffraction pattern is that of a single particle, but the intensity is the sum of all the diffraction patterns. Therefore, the diffraction pattern can be oversampled and the damage is distributed over all the particles. In this case, if enough particles can be aligned and passed through an X-ray beam (e.g. in the gas phase), atomic structures could be achieved on a conventional source by integrating the diffraction pattern long enough to accumulate the desired signal level. This is the best of both worlds: it gives a continuous diffraction pattern that eliminates, or at least ameliorates the phase problem, while it gives an integrated signal as large as crystals do.

There are simpler arrangements that approximate the ideal, but are easier to make. One possibility is a two-dimensional array of trays, of cages that is partly filled with well-oriented particles. A similar possibility is to fill the array with two kinds of particles, at least one of those being well oriented. The diffraction pattern of the empty trays has well-defined spots, and can therefore be subtracted.

4.2. Holography

Holography is one of the remedies for the phase problem of diffraction. In technical language, a hologram with a point-like reference has an analytic inversion formula. This property is in common with tomography. In contrast, the recovery of diffraction patterns does not have an inversion formula; even a well-oversampled diffraction pattern has to be recovered by iterations. Note that even when there is an inversion formula, the inversion itself is almost always ill posed.

Holographic reconstruction techniques are applicable for diffraction patterns if the diffracting particle has a known part. The waves diffracted by the known part are considered to be the holographic reference and the waves diffracted by the unknown part are the object waves. It has been amply demonstrated that such methods are effective even in crystallography.

5. Budget and Prioritization of Efforts

5.1. Budget

A summary of the budget of the LCLS biological imaging instrumentation and R&D is given below. In addition to the research and development outlined in Sec. 3, we need to consider the design, construction, and testing of the LCLS instrumentation itself. The research described in Sec. 3 does include vacuum chambers that will be used for validation experiments at synchrotrons, SPPS, and the VUV-FEL, as well as laboratory test stations, but has not included a dedicated chamber for LCLS. That chamber includes an injection system, particle-XFEL interaction diagnostics (fluorescence detection, mass spectrometry and electron spectrometry, visible microscope), and is estimated to cost $2,650K and 14 FTE of effort. In addition a biology support lab is required, with electron and visible microscopes, a wet-lab and a 120 Hz short-pulse laser ($2,500K, 3 FTE per year for 3 years). The totals of the LCLS instrumentation and laboratory is included in the summary below:

Optics:	17 FTEs and $1,550K
Particle delivery:	49 FTEs and $3,600K
Photon-matter interaction:	43 FTEs and $500K
Detector:	25 FTE and $6,500K
Reconstruction:	71 FTEs and $350K
LCLS Chamber and diag:	14 FTEs and $2,650K
Laboratory:	9 FTEs and $2,500K
Total:	228 FTEs and $17,650K

5.2. Outline of priorities

The plan to achieve atomic-resolution imaging at the LCLS in its first years of operations is a very ambitious one; many technologies need to be developed concurrently and implemented to achieve success. Some risks may be mitigated by following multiple

research tracks at several institutions, as in the case of particle injection and laser alignment. There is inherent uncertainty in planning any experiment at an XFEL source, since this high-peak-power regime has never yet been accessible experimentally. Much effort has been spent developing models of the interaction between particles and XFEL pulses, but these have not been validated. The uncertainty in the required pulse duration, for example, means that we must assume the worst case. Therefore, validation experiments, that can be carried out at the VUV-FEL, are of very high priority. Also, we have to investigate possible methods of pulse compression or slicing, and to plan to initially employ imaging techniques that will allow longer pulses. The plan of research during the first three years of LCLS operations should begin with measurements of the dynamics of particles exposed to the XFEL beam, and then move on to imaging particles with strong scattering signals (such as inorganic clusters) to demonstrate the technique and drive the injection technologies. This will be quickly followed by the imaging of biological material, such as membrane nanocrystals. Such experiments could significantly impact structural biology and will provide the research teams the required learning to move to 3D imaging of reproducible and laser-aligned particles.

A significant risk to single-particle diffraction imaging is the variability of structure from particle to particle, especially since the structure is not confined and/or selected by neighboring molecules as occurs in a crystal. Experimental evidence, for example mass spectrometry measurements of solvated proteins presented by Carol Robinson at the workshop, suggests a high degree of reproducibility, but more precise measurements are needed to quantify this. This problem can be addressed in part by large-scale molecular dynamics computations, and could also be experimentally examined by synchrotron-based X-ray scattering (radius of gyration) measurements of a cloud of molecules sprayed into vacuum. More precise measurements could be made if the molecules could be aligned. This provides further reason to rapidly develop laser alignment of biological molecules.

Since many groups will be developing components of the experiment in parallel, effective communication between groups is essential, as well as an understanding of the requirements and top-level design of the experiment. (That the community embraced this workshop as it did bodes well for this broad collaborative effort.) As pointed out in the sessions, a straw-man design of the entire experiment must be published so that all groups can work to a common goal.

Other priorities of significance include achieving near-theoretical signal to noise levels in the measurement of diffraction patterns. There will be many sources of noise that must be reduced, through careful experimental design and execution. Again, since there is no experience or wisdom in the community, there may be unexpected sources of noise. Sources of background scatter that must be considered include: coherent scattering from free electrons in the molecule; debris from the Coulomb explosion; Compton (inelastic) scattering; and scattering from gas molecules in the beam path. Other sources of noise include detector noise; stray radiation from the source; bremsstrahlung and fluorescence. In general the signal can be increased over the noise by averaging, although if the noise is too great this will reduce the achievable resolution to which diffraction patterns can be classified into the same orientations. Experiments at the VUV-FEL will provide learning to address this issue. Another issue that must be addressed promptly is the volume and rate of data that will be generated and the

processing required in order to reconstruct atomic structures from a series of millions of noisy diffraction patterns. While methods have been proposed for performing the averaging and classification, and 3D reconstruction, the entire process has not been carried out on such a dataset. On one hand, the challenge of the rate of data processing will be ameliorated by Moore's Law in that computers will be faster in five year's time. However, it is expected that parallel computing will be needed, and there is a large software and digital processing effort required (for example, for compressing the CCD signal to allow fast readout).

In summary, the three highest risks are the short timeline to LCLS experiments; the uncertainty of the pulse requirements for single-particle imaging; and the possible variability of structure from particle to particle. These are best addressed, respectively, by pursuing parallel tracks of research, especially in the area of particle handling; carrying out validation experiments at available sources such as the VUV-FEL and LCLS as soon as it is operational; and performing large-scale computations and X-ray diffraction measurements of laser-aligned molecules. The last effort obviously requires development of laser alignment.

Lower risks (with slightly lower priority than those listed above) include overcoming all sources of noise in the experiment to attain diffraction data close to that limited by photon shot noise; and being able to handle the large data stream (including the processing steps of classification and averaging, and image reconstruction).

6. Conclusions

Biological imaging at atomic resolution may well be the most challenging of all experiments that have been proposed for the LCLS. Nevertheless, there was an overwhelming consensus at the workshop that the benefits and potential of this experiment are so compelling that an aggressive and coordinated plan of research must be carried out by the community to carry this out. There are many unknowns to the experiment, but all aspects of the experiment do appear to be feasible with many of the key concepts being demonstrated experimentally or with detailed models. We now have a detailed understanding of what needs to be researched and developed in order to carry out biological imaging experiments at the LCLS. Just as importantly, we have a strong collaborative community with the necessary expertise to carry out this research. We believe that the key to success is in carrying out proof-of-principle experiments at available sources prior to LCLS operations, such as the VUV-FEL. Those experiments are designed to meet as many of the challenges as possible. In addition we will require a period of rapid learning once the LCLS begins operations. Such an effort will take diffraction imaging into the new regime provided by LCLS and will have a direct and lasting impact on this new field by building its foundations and shaping future research.

This work was performed under the auspices of the U.S. Department of Energy by the University of California, Lawrence Livermore National Laboratory under Contract No. W-7405-Eng-48.

Glossary of abbreviations

AFM:	Atomic Force Microscopy
ALS:	Advanced Light Source (at LBNL)
APS:	Active Pixel Sensor
BAMS:	Bioaerosol Mass Spectrometry
BER:	Office of Biological and Environmental Research
BES:	Office of Basic Energy Science
CCD:	Charge coupled detector
CMOS:	Complementary Metal Oxide Silicon
DESY:	Deutsches Elektronen-Synchrotron
DQE:	Detector Quantum Efficiency
ESI:	Electrospray ionization
ESRF:	European Synchrotron Radiation Facility
FPGA:	Field Programmable Gate Array
FTE:	Full-time equivalent (person year)
FWHM:	Full width at half maximum
IMS:	Ion Mobility Spectrometry
K-B:	Kirkpatrick-Baez (mirror pair for X-ray focusing)
LCLS:	Linac Coherent Light Source
MD:	Molecular Dynamics
MPI:	Max-Planck Institute
NIH NCRR	National Institutes of Health National Center for Research Resources
NSF:	National Science Foundation
PET:	Positron Emission Tomography
PIC:	Particle In Cell
PSF:	Point Spread Function
R&D:	Research and development
RMS:	Root mean squared
SAM:	Self-Assembled Monolayer
SEM:	Scanning Electron Microscopy
SLAC:	Stanford Linear Accelerator Center
SNAP:	Supernova / Acceleration Probe (see snap.lbl.gov)
SNR:	Signal to noise ratio
SPEDEN:	Single-Particle Electron Density (a computer programme)
SPIDER:	A single-particle reconstruction computer programme
SPN:	Scanned Probe Nanolithography
SPPS:	Sub-Picosecond Photon Source
SSRL:	Stanford Synchrotron Radiation Laboratory
STEM:	Scanning Transmission Electron Microscopy
TEM:	Transmission Electron Microscopy
TOF-MS:	Time of Flight Mass Spectrometry
VUV-FEL:	Vacuum Ultraviolet free-electron laser
XFEL:	X-ray free-electron laser

References

[1] http://www-ssrl.slac.stanford.edu/lcls/
[2] http://www-ssrl.slac.stanford.edu/lcls/papers/lclsii_besac_feb03.pdf
[3] O. Hignette, P. Cloetens, W.-K. Lee, W. Ludwig and G. Rostaing,
Hard X-ray microscopy with reflecting mirrors status and perspectives of the ESRF technology J. Phys. IV France 104 (2003) p. 231
[4] K. Yamauchi, K. Yamamura, H. Mimura, Y. Sano, S. Matsuyama, K. Ueno, M. Shibahara, K. Endo, M. Yabashi, K. Tamasaku, Y. Nishino, T. Ishikawa, Y. Mori, Fabrication technology of ultraprecise mirror optics to realize hard x-ray nanobeam, SPIE 5533-16
[5] Y. Mori, K. Yamauchi, K. Yamamura, H. Mimura, Y. Sano A. Saito K. Endo, A. Souvorov, M. Yabashi, K. Tamasaku, T. Ishikawa, Development of a figure correction method having spatial resolution close to 0.1mm, Proc. SPIE 5193, 105-111 (2004).
[6] Lin and Colwey, Ultramic 19, p. 31 (1986)
[7] H.N. Chapman, Wigner deconvolution X-ray microscopy, Ultramicros. 66, 153-172 (1996)
[8] H. N. Chapman, K. A. Nugent, X-ray pulse compression using strained crystals. [Journal Paper] Optics Communications 205, 351-9 (2002).
[9] P. Emma, K. Bane, M. Cornacchia, Z. Huang, H. Schlarb, G. Stupakov, and D. Walz, Femtosecond and Subfemtosecond X-Ray Pulses from a Self-Amplified Spontaneous-Emission Based Free-Electron Laser, Phys. Rev. Lett. 92, 074801 (2004).
[10] K. Fezzaa, F. Comin, S. Marchesini, R. Coisson and M. Belakhovsky, X-ray Interferometry using 2 coherent beams from Fresnel mirrors, Journal of X-rays Science and Technology 7, 12-23, (1997)
[11] J. J. A. Lin, D. Paterson, A. G. Peele, P. J. McMahon, C. T. Chantler, and K. A. Nugent “Measurement of the Spatial Coherence Function of Undulator Radiation using a Phase Mask”, Phys. Rev. Lett. 90, 074801 (2003)
[12] P. Cloetens, J. P. Guigay, C. DeMartino, et al. Fractional Talbot imaging of phase gratings with hard x rays Opt Lett 22, 1059-1061 (1997).
[13] Kohn V, Snigireva I, Snigirev A Direct measurement of transverse coherence length of hard x rays from interference fringes, Phys. Rev. Lett. 85, 2745 (2000)
[14] M. Yabashi, K. Tamasaku, and T. Ishikawa, “Characterization of the Transverse Coherence of Hard Synchrotron Radiation by Intensity Interferometry”, Phys. Rev. Lett. 87, 140801 (2001)
[15] M. Yabashi, K. Tamasaku, and T. Ishikawa, “Measurement of X-Ray Pulse Widths by Intensity Interferometry”, Phys. Rev. Lett. 88, 244801 (2002)
[16] Gaskell, S.J., "Electrospray: Principles and Practice", J. Mass Spectrom., 32, 677-688 (1997).
[17]Rostom, A.A., P. Fucini, D.R. Benjamin, R. Jueneman, K.H. Nierhaus, F.U. Hartl, C.M. Dobson, C.V. Robinson, "Detection and selective dissociation of intact ribosomes in a mass spectrometer", Proc. Natl. Acad. Sci. USA, 97, 5185-5190 (2000).
[18] Tito, M. A., Tars, K., Valegard, K., Hajdu, J., Robinson, C V. "Electrospray Time-of-Flight Mass Spectrometry of the Intact MS2 Virus Capsid," J. Am. Chem. Soc. 122, 3550-3551 (2000).
[19] Stephenson, J.L. and S.A. McLuckey, "Charge manipulation for improved mass determination of high-mass species and mixture components by electrospray mass spectrometry", J. Mass Spectrom. 33, 664-672 (1998).
[20] Stephenson, J.L. and S.A. McLuckey, "Charge manipulation for improved mass determination of high-mass species and mixture components by electrospray mass spectrometry", J. Mass Spectrom. 33, 664-672 (1998).
[21] Suess, D.T., K.A. Prather, "Mass Spectrometry of Aerosols", Chem. Rev. 99, 3007-3035 (1999).
[22] Bogan, M.J. and G.R. Agnes, "MALDI-TOF-MS analysis of droplets prepared in an electrodynamic balance:"wall-less" sample preparation", Anal. Chem., 74, 489-496 (2002).
[23] Fuerstenau, S.D. and W.H. Benner, "Molecular weight determination of megadalton DNA electrospray ions using charge detection time-of-flight mass spectrometry", Rapid Commun. Mass Spectrom. 9, 1528-1538 (1994)
[24] Benner, W. H., "A gated electrostatic ion trap to repetitiously measure the charge and m/z of large electrospray ions", Anal. Chem. 69, 4162-4168 (1997).
[25] D. G. Grier, "A revolution in optical manipulation," Nature 424, 810-816 (2003).

[26] R. Neutze, R. Wouts, D. v. d. Spoel, E. Weckert, J. Hajdu, Potential for biomolecular imaging with femtosecond x-ray pulses, Nature 406, 752-757 (2000).
[27] Z. Jurek, G. Faigel and M. Tegze, Dynamics in a cluster under the influence of intense femtosecond hard X-ray pulses, Eur. Phys. J. D 29, 217-229 (2004).
[28] S. P. Hau-Riege, R. A. London, A. Szoke, Dynamics of biological molecules irradiated by short x-ray pulses. Physical Review E. 69, 51906-1-12 (2004).
[29] SNAP Collaboration, to be published SPIE 4835, [arXiv:astro-ph/0209550].
[30] Meidinger N. Bonerz S. Eckhardt R. Englhauser J. Hartmann R. Hasinger G. Holl P. Krause N. Lutz G. Richter R. Soltau H. Struder L. Trumper J., First measurements with a frame store PN-CCD X-ray detector Source, Nuclear Instruments & Methods in Physics Research Section A-Accelerators Spectrometers Detectors & Associated Equipment. 512(1-2):341-349, (2003).
[31] Mueller, F., Sommer, I., Baranov, P., Matadeen, R., Stoldt, M., Wohnert, J., Gorlach, M., van Heel, M., Brimacombe, R., The 3D arrangement of the 23 S and 5 S rRNA in the Escherichia coli 50 S ribosomal subunit based on a cryo-electron microscopic reconstruction at 7.5 Å resolution. J. Mol. Biol. 298, 35–39 (2000).
[32] Saxton, W.O., Frank, J., Motif detection in quantum noiselimited electron micrographs by cross-correlation. Ultramicroscopy 2, 219–227, (1977).
[33] van Heel, M., Angular reconstitution: a posteriori assignment of projection directions for 3D reconstruction. Ultramicroscopy 21, 111–124, (1987).
[34] J. R. Fienup, Phase retrieval algorithms: a comparison, Appl. Opt. 21, 2758-2769 (1982).
[35] S. Marchesini, H. He, H. N. Chapman, S. P. Hau-Riege, A. Noy, M. R. Howells, U. Weierstall, J.C.H. Spence, X-ray image reconstruction from a diffraction pattern alone, Phys. Rev. B 68, 140101(R) (2003)
[36] S. P. Hau-Riege, H. Szoke, H. N. Chapman, A. Szoke, S. Marchesini, A. Noy, H. He, M. R. Howells, U. Weierstall, J. C. H. Spence, SPEDEN: Reconstructing single particles from their diffraction patterns, Acta Cryst. A60, 294-305 (2004).

A. Workshop Agenda

AGENDA

Instrument Development Workshop for Biological Imaging Experiments at LCLS, 15-16 March 2004

Research Office Building, Meeting Room ABCD
Stanford Linear Accelerator Center
Menlo Park, CA 94025

Monday, 15 March

08:00-09:00	*BREAKFAST AND REGISTRATION*	
09:00-09:15	**Welcome, LCLS overview, instrumentation for biology, scope of workshop** H. Chapman, LLNL, K. Hodgson,SLAC/SSRL, Janos Hajdu, Uppsala	
09:15-09:30	**SPPS, a status report**	Jerry Hastings, SLAC/SSRL
09:30-10:30	**Front-end optics** Directed discussion	Discussion leader: John Arthur, SLAC/SSRL
10:30-10:45	*COFFEE BREAK and discussion*	
10:45-12:00	**Particle delivery systems and orientation**	Discussion leader:
	Mass-spec injection Directed discussion	C. Robinson, Cambridge
12:00-13:00	*WORKING LUNCH*	
13:00-14:00	**High-energy density photon-matter interactions** Dick Lee, LLNL	Discussion leader:
	Overview of damage models Directed discussion	R. London, LLNL
14:00-15:00	**Detectors and diagnostics**	Discussion leader: Howard Padmore, LLBL
	Pixel detectors Directed discussion	G. Derbyshire, CLRC

15:00-15:30	*COFFEE BREAK and discussion*	
15:30-16:30	**Reconstruction computations**	Discussion leader: Henry Chapman, LLNL
	Reconstruction algorithms Directed discussion	V. Elser, Cornell (tentative)
16:30-17:30	**Alternative methods**	Discussion leader: Simone Techert, Max Planck Goettingen
17:30-	*BARBEQUE DINNER (onsite)*	

AGENDA – DAY 2

Instrument Development Workshop
for Biological Imaging Experiments at LCLS, 15-16 March 2004

Research Office Building, Meeting Room ABCD
Stanford Linear Accelerator Center
Menlo Park, CA 94025

Tuesday, 16 March

08:00-09:00	*BREAKFAST and discussion*	
8:30-9:30	**Identification and prioritization of risks and efforts**	Dennis Matthews, CBST
9:30-9:45	**Instructions for breakout sessions**	
9:45-11:30	**Breakout sessions** – write 2-page statement of need (coffee provided)	
11:30-12:00	**Reconvene, report, wrap-up**	
	END OF MEETING	

B. Workshop Participants

ATTENDEE	AFFILIATION	E-MAIL	AREA OF EXPERTISE
Organisers			
Keith Hodgson	SLAC/SSRL	hodgson@ssrl.slac.stanford.edu	sources/imaging
Henry Chapman	LLNL	henry.chapman@llnl.gov	damage/imaging
Janos Hajdu	Uppsala Univ.	janos@xray.bmc.uu.se	damage/imaging
Invited speakers			
Jerry Hastings	SLAC/SSRL	jbh@ssrl.slac.stanford.edu	sources
Carol Robinson	Cambridge Univ.	cvr24@cam.ac.uk	mass spec/particle handling
Matthias Frank	LLNL	frank1@llnl.gov	particle injection
Musa Ahmed	LBNL	mahmed@lbl.gov	particle injection
Howard Padmore	LBNL	hapadmore@lbl.gov	detectors
Soichi Wakatsuki	KEK	soichi.wakatsuki@kek.jp	detectors/sources
Gareth Derbyshire	CLRC	G.E.Derbyshire@rl.ac.uk	detectors
Richard Lee	LLNL	dicklee@physics.berkeley.edu	damage
Richard London	LLNL	rlondon@llnl.gov	damage
Henry Chapman	LLNL	henry.chapman@llnl.gov	imaging
Janos Hajdu	Uppsala	janos@xray.bmc.uu.se	damage/imaging
Abraham Szoke	LLNL	szoke1@llnl.gov	damage/reconstruction
Veit Elser	Cornell	ve10@cornell.edu	reconstruction
Alan Wootton	LLNL	wootton1@llnl.gov	optics
John Arthur	SLAC/SSRL	jarthur@ssrl.slac.stanford.edu	optics/sources
Simone Techert	Max-Planck	stecher@gwdg.de	time resolved
Keith Hodgson	SLAC/SSRL	hodgson@ssrl.slac.stanford.edu	sources/imaging
Phil Anfinrud	NIH/NIDDK	anfinrud@helix.nih.gov	time resolved
Dennis Matthews	CBST	dmatthews@llnl.gov	biological aspects
Discussion leaders			
Matthias Frank	LLNL	frank1@llnl.gov	particle injection
Henry Chapman	LLNL	henry.chapman@llnl.gov	damage/imaging
Alan Wootton	LLNL	wootton1@llnl.gov	optics
Richard Lee	LLNL	dicklee@physics.berkeley.edu	damage
Howard Padmore	LBNL	hapadmore@lbl.gov	detectors
Keith Hodgson	SLAC/SSRL	hodgson@ssrl.slac.stanford.edu	sources/imaging
Janos Hajdu	Uppsala Univ.	janos@xray.bmc.uu.se	damage/imaging
John Arthur	SLAC/SSRL	jarthur@ssrl.slac.stanford.edu	optics/sources
Simone Techert	Max-Planck	stecher@gwdg.de	time resolved
Kelly Gaffney	Stanford	kgaffney@ssrl.slac.stanford.edu	ultrashort lasers
Dennis Matthews	CBST	dmatthews@llnl.gov	biological aspects
Participants			
Calle Caleman	Uppsala Univ.	calle@xray.bmc.uu.se	damage
Magnus Bergh	Uppsala Univ.	magnus@xray.bmc.uu.se	damage
Stefan Hau-Riege	LLNL	hauriege1@llnl.gov	damage/imaging
Roger Falcone	UC Berkeley	rfalcone@socrates.Berkeley.EDU	short-pulse sources
Hope Ishii	LLNL	ishii2@llnl.gov	imaging
Gosta Huldt	Uppsala Univ.	huldt@xray.bmc.uu.se	reconstruction
Stefano Marchesini	LLNL	smarchesini@llnl.gov	reconstruction

Jim Fienup	U. Rochester	fienup@optics.rochester.edu	reconstruction
Ken Downing	LBNL	KHDowning@lbl.gov	Cryo-EM
Malcolm Howells	LBNL	MRHowells@lbl.gov	reconstruction/optics
David Sayre	Stony Brook U.	sayre@xray1.physics.sunysb.edu	reconstruction
Eugene Ingerman	UC Davis	eugening@math.berkeley.edu	reconstruction
Uwe Weierstall	ASU	UWE.WEIERSTALL@asu.edu	reconstruction
Ingolf Lindau	SLAC/SSRL	lindau@ssrl.slac.stanford.edu	sources
Max Cornacchia	SLAC/SSRL	cornacchia@ssrl.slac.stanford.edu	sources
Keith Nugent	U. Melbourne	K.Nugent@physics.unimelb.edu.au	optics/reconstruction
John Galayda	SLAC/SSRL	galayda@ssrl.slac.stanford.edu	sources
Ian McNulty	ANL	mcnulty@aps.anl.gov	optics/reconstruction
Aleksandr Noy	LLNL	noy1@llnl.gov	samples
Daniel Barsky	LLNL	barsky1@llnl.gov	structural biol
Henry Benner	LLNL	benner2@llnl.gov	sample injection
Brent Segelke	LLNL	segelke1@llnl.gov	sample preparation
John Spence	Arizona State U.	spence@asu.edu	reconstruction
Bill Weis	Stanford	bill.weis@stanford.edu	structural biol
Janos Kirz	Stony Brook U.	kirz@sbhep.physics.sunysb.edu	reconstruction/optics
Rodney Balhorn	LLNL	balhorn2@llnl.gov	biology
Friedrich Schotte	NIH/NIDDK	FriedrichS@intra.niddk.nih.gov	time-resolved
Britt Hedman	SLAC/SSRL	hedman@ssrl.slac.stanford.edu	alternatives
Sol Gruner	Cornell	smg26@cornell.edu	detectors
Steve Lane	CBST	slane@llnl.gov	imaging
John Sedat	UCSF	sedat@msg.ucsf.edu	reconstruction
David Shapiro	Stony Brook U.	davishap@yahoo.com	reconstruction
Enju Lima	Stony Brook U.	lima@xray1.physics.sunysb.edu	reconstruction
Bruce Doak	ASU	bdoak@asu.edu	EM/imaging